Model-free based control of a gripper actuated by pneumatic muscles

Pol Hamon, Loïc Michel, Franck Plestan, Damien Chablat

Model-free based control of a gripper actuated by pneumatic muscles[1]

Pol Hamon[a,b], Loic Michel[a], Franck Plestan[a], Damien Chablat[a,c]

[a] *Nantes Universite, Ecole Centrale Nantes, CNRS, LS2N, UMR 6004, City One, F-44000, France*
[b] *Armor Meca, ZI La Grignardais, Pleslin-Trigavou, 22490, France*
[c] *Technical University of Cluj-Napoca, Strada Memorandumului 28, Cluj-Napoca, 400114, Roumania*

Abstract

In this article, a model-free based control strategy is applied to a gripper activated by Mckibben's pneumatic muscles. The gripper is composed of three fingers and is based on an original mechanical design to grip a large range of objects (by a weight, size, form, ... point-of-view). A model-free based control strategy is proposed to manage the force control phases. An experimental setup is introduced to experimentally test and validate the proposed control strategy using a very simple setup composed of a single force sensor, an embedded electronic board, and a single pressure proportional solenoid valve.

Keywords: Grasping system, pneumatic muscle, model-free control.

1. Introduction

One of the great challenges of industrial robotics is to manipulate safely a large number of objects with varied and complex shapes and different masses. For this reason, a new under-actuated hand has been developed [1], each finger being mechanically designed to be adaptable to a large range of objects. Nowadays, no other under-actuated finger uses a spherical parallel joint at the base of the finger to provide abduction movement [2]. This allows to switch easily between cylindrical and spherical grasping. The original design of the fingers is unique to the authors; actually, no other author uses a spherical parallel joint at the base of the finger to provide abduction movement. To actuate this new mechanical architecture, pneumatic muscles have been chosen since the coupling between pressure, contraction, and effort can be advantageous to achieve under-actuated gripping [3]. Furthermore, the high effort-mass ratio of pneumatic muscles is an interesting feature when an object is grabbed. Notice that motion-pressure nonlinearities are advantageous to ensure the stability of the efforts between the fingers applied on the object [4].

The transition from free fingers motion to holding the object is intuitive. There are two very different situations, which use two kinds of feedback: proprioception and touch. In the human case, the vision allows anticipating the transition between these two situations. In the current work, it is stated that there is no visual information; an intuitive blind grasp has to be recreated. Sensors based solutions have been proposed in [5, 6], switching between the motion phase and the grasping phase. However, these solutions introduce the problem of reliable and responsive contact detection; as an example, in [7], fuzzy logic is used for a smooth transition between the two sensors.

[1] A preliminary version has been published in the proceedings of 9^{th} IFAC Symposium on Mechatronic Systems, Los Angeles, California, USA, 2022.

The solution introduced in the current paper introduces an alternative to this problem by using a well-matched reference trajectory. Indeed, a solution for a gripper including force control without contact detection is proposed.

As previously mentioned, the gripper under interest is actuated by a Mckibben pneumatic muscle. Few contributions have been made about the control of pneumatic artificial muscles (PAM) used as actuators [8, 9] for a finger. Standard Ziegler-Nichols method has been proposed in [10] to tune a PID position controller. Similarly, a PID controller tuned by the Simulated Annealing method has been considered in [11] regarding a positioning system. In [12], an experimental PID control based on a specific hysteresis model has been proposed. Such strategies require the identification of a model: thus, self-identification-based control using neural networks has been proposed in [13, 14, 15, 16]. A recent contribution to illustrate the feasibility of a positioning system using a grey-box-based identification modelling using neural networks and sliding mode control in real-time applications has been proposed in [17].

In this paper, the objective is to design a control strategy for the gripper requiring a very reduced effort for the identification process. Furthermore, it is necessary to get a sufficient robustness versus the mass and shape of the objects. So, a model-free based effort control is selected. Based on authors' previous work [18], a model-free control strategy [19] is proposed to solve the problem of controlling the motion of a gripper actuated by pneumatic muscles, for grasping a wide variety of different objects, while limiting the identification process. The model-free control approach [20] can be considered as an alternative to the standard PI and PID controls; it does not require any prior knowledge of the plant, and it is straightforward to tune. Its usefulness has been demonstrated in many situations through successful applications (for details, see [21, 19, 22]). In particular, some applications to mechanical systems have been dedicated to the control of quadrotor position [23, 24], control of machine tool positioning systems [25], position control of a cable-driven parallel robot [26], or control of electro-active polymer actuators [27]. Notice that this kind of control approach is computationally efficient, easily deployed even on small embedded devices, and can be implemented in real-time since it requires very light computations.
One additional novelty of the present study lies in the utilization of a non-hybrid control law, which eliminates the need for contact sensors or position sensors on every joint. Instead, it relies on a single effort feedback measurement. This approach capitalizes on the significant nonlinear characteristics exhibited by the effort and displacement dynamics of the pneumatic muscle. As a result, it enables the gripper to reach a stable position without requiring prior knowledge of the object's shape. In summary, the main contributions and novelties of this work can be summarized as follows.

- The mechanical characteristics of the gripper, specifically the spatial displacements of the fingers (flexion and abduction), as well as its actuation through the utilization of pneumatic muscles.
- The adoption of a non-hybrid control structure that eliminates the need for contact detection.
- The implementation of a model-free based control approach that necessitates only a minimal amount of modelling knowledge, thereby reducing the requirement for an extensive identification process.

The novelty of this mechanical gripper design primarily lies in its finger spatial displacements, which are accomplished using a single actuator powered by a pneumatic muscle [1]. This single

actuator is capable of controlling both the flexion and abduction movements of the fingers. Another notable innovation is the utilization of a single valve to regulate the pressure injected into the three muscles. This design assumes that the gripper naturally reaches a mechanical equilibrium point that enables it to securely grasp and hold objects.

The paper is structured as follows. Section 2 states the control problem during grasping tasks, especially the design of a unique reference trajectory without formal contact detection. In Section 3, principles of model-free control are recalled. Section 4 presents the experimental setup, which is composed of a hand with three fingers actuated by three pneumatic muscles, as well as experimental results and discussion.

2. Description of the system and control problem statement

2.1. Mock-up of three-fingers hand

Figure 1-left presents a mock-up of the under-actuated 12 degrees of freedom robotics hand with three under-actuated fingers [28]. The proximal phalange is formed by the two opposite bars of the spherical parallel mechanism represented in yellow, and the middle and distal phalanges are represented in orange and red, respectively. Two 4-bar mechanisms represented in blue and green allow the transmission of the movement produced by the pneumatic muscle on the phalanges. Each finger performs spatial motions to achieve more complex and varied grasping than the existing planar-movement fingers and is actuated by one pneumatic muscle. The purpose of this hand is to grasp a wide range of complex-shaped objects at the exit of machining centers, the objects being of different sizes, shapes, and weights. Its kinematics allows these properties (for details, the reader can refer to [28]).

The main industrial objective guiding the design of this hand is linked to ensured and safe grasping. The industrial application does not require fast grasping to preserve the quality of the surface. Furthermore, the industrial context requires constraints on sensors (low price, reduced number, ...). Notice that the wide range of objects induces the design of a robust control strategy in order to have no tuning procedure for each part. Furthermore, given the difficulty to get a control-oriented modeling of the system, a so-called model-free controller is designed in the sequel.

The paper is a first step to validate the gripper model free based control; thus, the control design is made under some hypotheses:

- **Assumption 1.** A similar control is applied to the three muscles (and then, to the three fingers). As a consequence, the velocity of the motion of each finger is consequently the same during the approach phase with the object;
- **Assumption 2.** Only one finger is equipped by a force sensor, this latter sending the single measurement to the controller;
- **Assumption 3.** The contact with the object is made at the same time for the three fingers.

2.2. Closing and opening phases

The description of the different phases of a gripping cycle with the gripper displayed in Figure 1-left is presented in the sequel (see Figure 1-right); these phases allow first to grasp the object, then to release it.

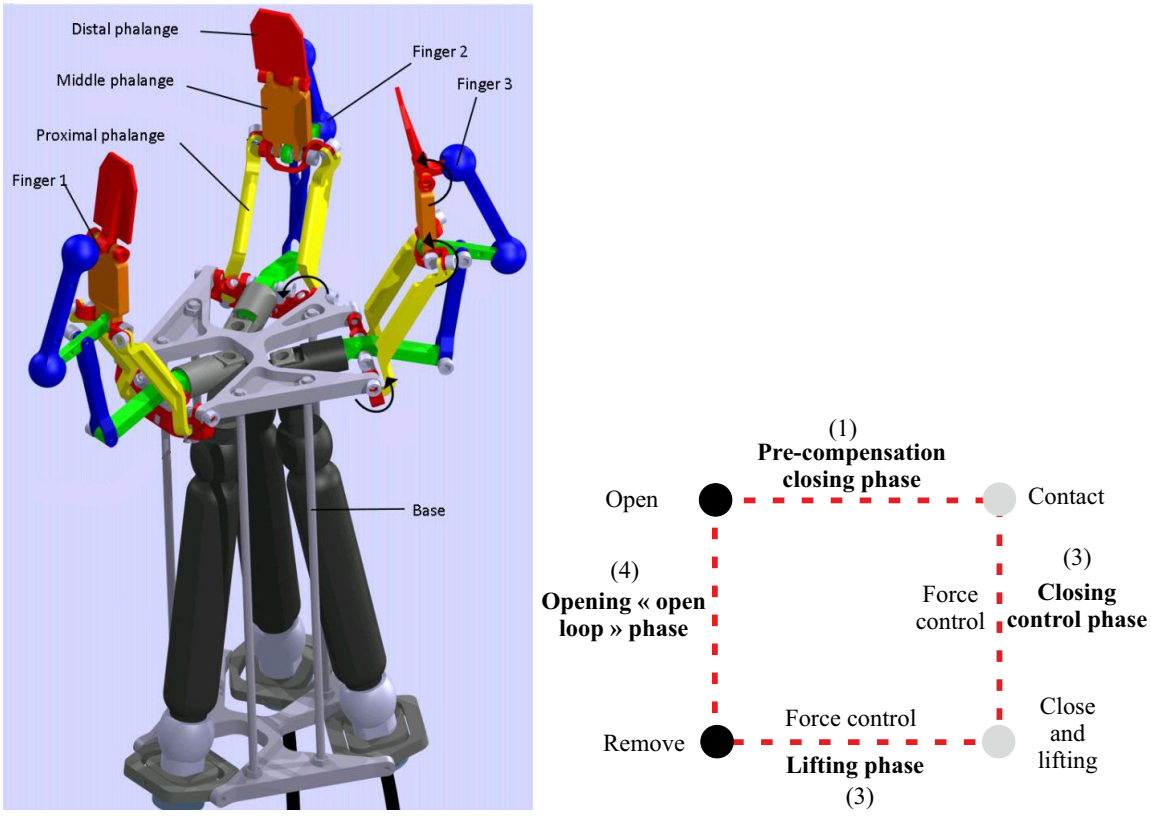

Figure 1: **Left.** Kinematics of the under-actuated gripper architecture with a spherical parallel mechanism [28]. **Right** Phases for grasping/releasing an object.

- **Phase 1.** There is no contact. The objective is to generate a motion of the three fingers to obtain contact with the object; the goal is to achieve a given force when contact between the fingers and the object appears. However, during this phase during which there is no contact, it is not possible to act on the force. The challenge is to define a reference trajectory allowing to reach a given force, at a contact time unknown *a priori* and with a constant zero force during all the phases. This reference trajectory which is a key point of the control strategy will be detailed in the sequel.
- **Phase 2.** The contact is established. The objective is then to control the contact force in order to maintain the object in the hand[2].
- **Phase 3.** The support of the object is removed; the grasping has to keep the object maintained by opposing the gravity force. In this phase, the force control must be robust given the variation of gravity force.
- **Phase 4.** The gripper is opened. As a consequence, the contact is broken. A specific strategy is applied to limit the velocity of the fingers, the aim being to reduce the risk of collision with other objects.

2.3. A unique reference trajectory for phases 1, 2 and 3

The objective is the design of a reference trajectory allowing, without formal contact detection, to track a unique trajectory over Phases 1, 2, and 3. The interest of a single reference trajectory without contact detection is the continuity of the trajectory; furthermore, contact detection can be tricky due to the presence of noise on low-cost sensors and could induce a back-and-forth between Phases 1 and 2. In fact, the reference trajectory definition and the control problem must take into account several constraints:

- the trajectory is unique for pre-contact (Phase 1) and contact phases (Phases 1 and 2) and no formal detection is made;
- the velocity of the fingers tips must be limited in order to limit the overshoot when the desired force is obtained. The overshoot limitation is important to ensure a safe grasping of the object;
- during the pre-contact phase (Phase 1), the system is not controllable given that there is no contact, hence the force keeps zero during the motion.

Denote y^* the *desired force* and y^r the *reference trajectory* that are defined through a precompensator (see Figure 2) and reads as

$$y^r = (1 - K\sigma(t))y^* + Ky \tag{1}$$

with y the measured force applied to a single fingertip. The function $\sigma(t)$ is a monotonically increasing continuous one defined such that $\sigma(0) \geq 0$ is small and $\sigma(t \to \infty) = 1$. The parameter K is such that $0 < K < 1$. Denoting $e = y^r - y$ the tracking error and recalling that y (the measured force applied to a fingertip) keeps 0 between the initial and contact times, one has

[2]Recall here the assumption of the above section: the contact of each finger with the object is supposed to be active at the same instant. Hence, the force measured by the dedicated finger is related to the velocity of the approaching phase as well as the equilibrium point of the resulting forces that are distributed among the fingers during the phase of contact.

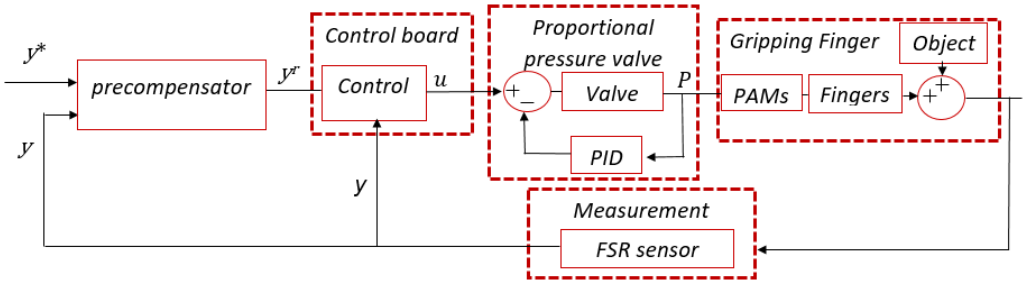

Figure 2: Closed-loop scheme including a pre-compensation of the desired trajectory: y is the measured force, y^* is the desired reference trajectory, and y_r is the reference trajectory defined by (1).

- for $t = 0$, $\sigma(0) = 0$, $y = 0$, then $e = y^*$;
- for $0 < t < t_c$ with t_c being the first contact instant, then

$$e = (1 - K\sigma(t))y^* \tag{2}$$

  In this case, the tracking error is naturally decreasing as $\sigma(t)$ is increasing. Notice that the control still has no action on the tracking error given that there is no contact, *i.e.* $y = 0$ for all $t \in [0, t_c)$, but this strategy reduces the error. It will allow a lower magnitude of the control at the contact time, a lower contact velocity between the fingertips and the object, hence a reduced force overshoot.

- for $t \geq t_c$, the tracking error reads as

$$e = (1 - K\sigma(t))y^* - (1 - K)y \tag{3}$$

  Given that $\sigma(t)$ converges to 1, it yields $e = (1-K)\cdot(y^*-y)$. So, the control forces e towards 0, inducing $y \to y^*$.

Figure 2 summarizes the closed-loop scheme with the desired trajectory y^* as input. The reference trajectory y^r is computed by the precompensator (1). The force y, defined as the output of the system, is measured and controlled via the control board system. A single proportional pressure valve (see details in Section 4) allows injecting a controlled pressure, driven by the control board, inside the three pneumatic muscles.

2.4. About the controllability of the force

As shown in Figure 2, the proposed control system of the fingers is based on a closed-loop for which the purpose is to control the contact force with the object. A particularity of this system is that the measured force y equals zero during Phase 1 since the fingers move to hang the object. From the control point of view, it highlights the fact that the system is not controllable during Phase 1, since the control input has no effect on the output y.

Furthermore, the definition of reference trajectory y^r consists in imposing progressively a pressure to the muscle in order to create a smooth contact with the object and allows "switching" the control law between Phases 1 and 2.

3. Control design based on model-free approach

As previously introduced, the objective is to propose a new control scheme that requires a very reduced effort for the identification/modeling while keeping high performances in terms of accuracy and robustness. A solution is the so-called "model-free control" approach that is detailed in [19]. The corresponding "intelligent" controllers are much easier to implement and tune than PID controllers, which are now the main tools in industrial control engineering (for example, see [29]).

3.1. The ultra-local model

The main ideas of model-free control are explained in the sequel. This approach is based on an ultra-local model in the sense that it is well-adapted during a very short time. From this ultra-model, a linear controller is designed. A key point is the capability of the controller to be adapted to the evolution of this ultra-local model given that very reduced information on the system is required.

Consider that the dynamic modeling of the plant[3] is made by a following first order *ultra-local model* which reads as

$$\dot{y} = F + \alpha u \tag{4}$$

where

- y and u are respectively the control and output of the system;
- the term F includes all the nonlinearities, disturbances, uncertainties, ...;
- $\alpha \in \mathbb{R}$ is a constant chosen by the practitioner such that $\dot{y}$ and αu are of the same magnitude. Therefore, α does not need to be precisely estimated.

As previously mentioned, equation (4) is only valid during a short time-lapse, hence the *ultra-local* term that must be continuously updated.

3.2. Control design

As a trivial introduction, supposing that F is *perfectly known* and considering the following controller

$$u = -\frac{F - \dot{y}^r}{\alpha} - K_p e \tag{5}$$

where y^r is the output reference trajectory (assumed to be well-known), $e = y - y^r$ is the tracking error, and $K_p > 0$ is a tuning gain[4], then the closed-loop system behavior is governed by the following equation

$$\dot{y} = \dot{y}^r - \alpha K_p e \tag{6}$$

that gives $\dot{e} = -\alpha K_P e$. However, F is unavailable; considering another control strategy is then required. A solution called "intelligent" digital P-controller [19] can be derived. To make an accurate analysis and given that the control law will be implemented in discrete time, a discrete version of the control input is considered in the sequel. Defining the sampling time h and $t_k = k \cdot h$

[3] For sake of simplicity and clarity, the system is supposed to be a SISO (single-input single-output) one.

[4] Practically, α and K_p can be tuned following e.g. the proposed procedure described in [30].

being the k^{th} sampling time at which the control and output are updated, the discrete version of (5) reads as

$$u_k = -\frac{F_{k-1}}{\alpha} + \frac{1}{\alpha}\frac{\Delta y^r|_k}{h} - K_p e|_k \tag{7}$$

with $\Delta y^r|_k = y_k^r - y_{k-1}^r$ and $e|_k = y_k - y_k^r$ the tracking error between the measurement y_k and its reference trajectory y_k^r at $t = t_k$. The unknown term F_{k-1} is estimated as described in the sequel from the previous measurement y_{k-1} and the control output u_{k-1}. Indeed, an approximation of the ultra-local model (4) at $t = t_{k-1}$ reads as (with $\Delta y|_{k-1} = y_{k-1} - y_{k-2}$)

$$\frac{1}{h}\,\Delta y|_{k-1} = F_{k-1} + \alpha u_{k-1} \tag{8}$$

and gives

$$F_{k-1} = \frac{1}{h}\,\Delta y|_{k-1} - \alpha u_{k-1} \tag{9}$$

Substituting (8) into (7) leads in the direct transposition of (5) into the discrete time domain that reads

$$u_k = -\frac{1}{\alpha}\left(\frac{1}{h}\,\Delta y|_{k-1} - \alpha u_{k-1}\right) + \frac{1}{\alpha}\frac{\Delta y^r|_k}{h} - K_p e|_k \tag{10}$$

that gives

$$u_k = u_{k-1} - \frac{1}{\alpha}\left(\left.\frac{\Delta y}{h}\right|_{k-1} - \left.\frac{\Delta y^r}{h}\right|_k\right) - K_p(y|_k - y^r|_k) \tag{11}$$

Regarding the implementation purpose, equation (11) is rewritten as

$$u_k = u_{k-1} - \frac{1}{\alpha h}\left(\Delta y|_{k-1} - \Delta y^r|_k\right) - K_p(y|_k - y^r|_k) \tag{12}$$

where $\frac{1}{\alpha h}$ adjusts the weight of the derivative / anticipation part while K_p adjusts the weight of the proportional part. This proportional part acts as the main "amplification" that forces the asymptotic error reduction; both parameters are involved in the transient dynamic behaviour which can be slightly accelerated using a higher anticipation, while keeping lower gain K_p prevents from entering into saturation or unstable behaviour.
The convergence behaviour of the closed-loop system can be established as described in the sequel. Considering the ultra-local model (8) at $t = t_k$

$$\left.\frac{\Delta y}{h}\right|_{k-1} = F_{k-1} + \alpha u_{k-1} \tag{13}$$

One gets

$$u_{k-1} = \frac{1}{\alpha}\left(\left.\frac{\Delta y}{h}\right|_{k-1} - F_{k-1}\right) \tag{14}$$

Replacing (14) in (11), one gets

$$u_k = \frac{1}{\alpha}\left(\left.\frac{\Delta y}{h}\right|_{k-1} - F_{k-1}\right) - \frac{1}{\alpha}\left(\left.\frac{\Delta y}{h}\right|_{k-1} - \left.\frac{\Delta y^r}{h}\right|_k\right) - K_p(y|_k - y^r|_k) \tag{15}$$

Multiplying (15) by α gives

$$\alpha u_k = -F_{k-1} + \left.\frac{\Delta y^r}{h}\right|_k - \alpha K_p(y|_k - y^r|_k) \tag{16}$$

Since (from (8)) one has

$$\alpha u_k = \left.\frac{\Delta y}{h}\right|_k - F_k, \tag{17}$$

one gets

$$\left.\frac{\Delta y}{h}\right|_k - F_k = -F_{k-1} + \left.\frac{\Delta y^r}{h}\right|_k - \alpha K_p(y|_k - y^r|_k) \tag{18}$$

that gives

$$\left.\frac{\Delta y}{h}\right|_k - \left.\frac{\Delta y^r}{h}\right|_k = (F_k - F_{k-1}) - \alpha K_p(y|_k - y^r|_k) \tag{19}$$

Assumption 4. The ultra-local model is valid only over a very short time during which the perturbation is such that $F_k \approx F_{k-1}$.

From this latter assumption and (19), it implies that the error e converges towards 0. Notice that,

- as previously discussed, both α and K_p are associated to the dynamic rate of the convergence;
- the previous assumption requires a relatively small sampling period.

Remarks.

- The presence of u_{k-1} in the definition of u_k allows, by an indirect way, to take into account the unknown term F_{k-1}.
- The control law (12) requires a numerical time derivation of y. Its estimation is made using a differentiator based on the Euler methodology. Consider the following assumption

Assumption 5. The output y (that is, in this work, the force applied to the tip of one finger) is differentiable.

- To manage both phases, the reference trajectory should be chosen smoothly given the presence of the derivative of $y^r(t)$ in (12).

4. Experimental setup for a prototype three-finger gripper

This section is devoted to the application of a model-free based control strategy to spatial kinematics of under-actuated fingers developed for spherical and cylindrical grasps. This kinematics is characterized by the integration of a spherical parallel mechanism in the proximal phalanx [1] and generalizes the work on the under-actuated fingers [2]. This solution (see Figure 1) provides non-planar behavior in relation to the abduction movements of the human hand and thus a change in the type of grasping. Some features have to be mentioned (for details, see [28])

- each finger has four degrees of freedom which are not directly controlled by the actuator, whose behavior depends on the contact between the fingers and the object;
- all joints are passive without angular position sensors, except for the prismatic joint that operates with a Mckibben pneumatic muscle. Small torsional springs are placed on the passive joints in order to return to the home position.

- to decrease the number of elements, the smallest number of fingers is used to take spherical and prismatic objects. So, the robotic hand is composed of three under-actuated fingers whose placement is defined to reach the two types of handles: prismatic and spherical.

Model-free control strategies apply very well to this type of mechanism because it is a hard task to model the dynamic behavior of the under-actuated fingers as well as the interactions between the fingers and the object (the contact points between the object and the phalanges are not known). Furthermore, the actuation choice based on pneumatic muscles increases the modeling challenge, as these actuators are highly nonlinear and uncertain.

The experimental setup is displayed in Figure 3, and its main elements begin detailed in the sequel.

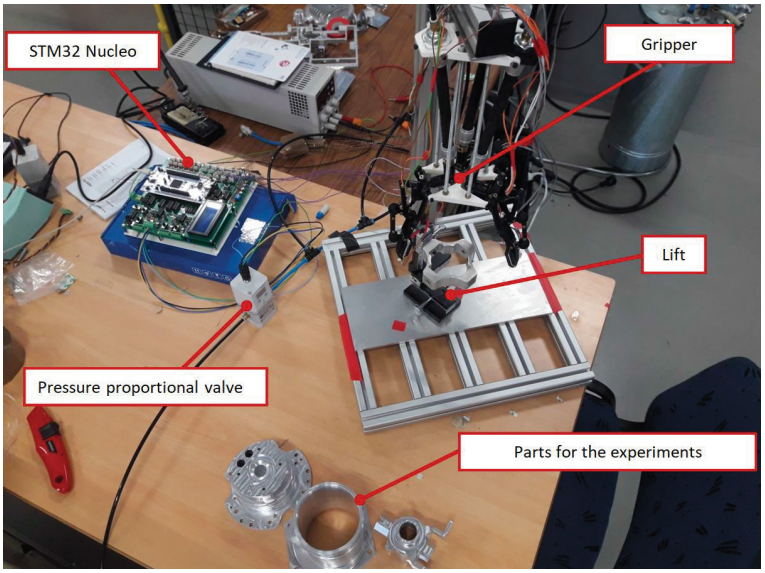

Figure 3: Photo of the whole experimental setup with an STM32 Nucleo board, a pressure proportional valve, and the gripper.

4.1. Pressure proportional valve

The control signal (see Figure 2) is sent to a FESTO VPPE [5] pressure proportional solenoid valve that transmits pressure to the three Mckibbens muscles of the hand (DMSP AM-CM 10 130N[6]). The valve is controlled by a $4-20$ mA signal with 2700 resolution points. The use of this type of valve makes it possible not to use PWM in the control and thus not to stress the muscle in frequency.

4.2. Contact forces measurement

In this paper, the measurement system has been integrated into the distal phalange (see Figure 4) of a single finger. The force relationship applied by the three fingers on the object depends on the shape of the object. Given that, in the case study, the shape is unknown, a single control is

[5]Data-sheet: `https://www.festo.com/tw/en/a/8114536/`
[6]Data-sheet: `https://www.festo.com/media/pim/555/D15000100140555.PDF`

applied to the three fingers and a single contact information is available, it is necessary to consider only symmetrical objects. Future works will study the case of asymmetrical objects that will have consequence on the control scheme.

Recall that the force measurement is not operating during Phase 1 given that there is no contact between the fingertip and the object. Concerning the measurement system, for the mechanical stability of the contact surface, two FSR force sensors (IE FSR X 402) are used between the polymer/aluminum contact surface and the finger (Figure 4). These two sensors return 0-5V analog signals that are summed to obtain the contact force signal. The latter is filtered using a standard Butterworth filter 20 Hz-fourth order.

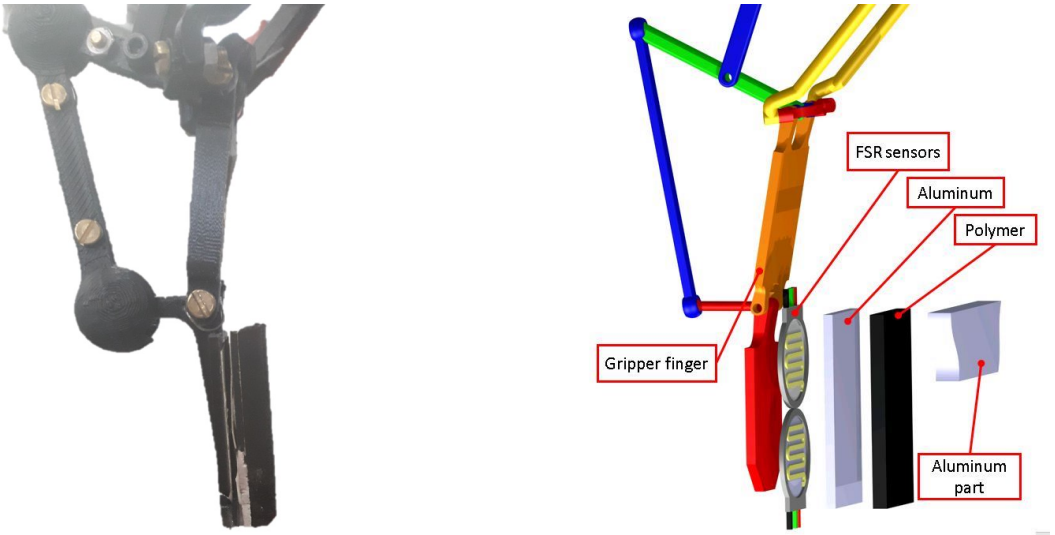

(a) (b)

Figure 4: Integration of force sensors on the distal phalange.

4.3. Experimental results and discussion

The ability to forcefully control the gripper is tested in various grip configurations, as presented in the literature with an egg [2]; thereafter, only Phases 1-3 are considered. Notice that the object is placed on a support that is removed once the grip is over.

The coefficient α has been tuned as $2.5.10^7$, which allows a reasonable dynamics for the pressure and the force. The coefficient $K_p = 8.10^{-3}$ has been chosen in order to avoid control saturation while keeping good static/dynamic performances. The coefficient K may slow down the closing of the hand in order to avoid a strong overshoot of the force that increases at the contact instant between the finger with the object (see Section 4.5 for a more detailed study of the precompensator characteristics). Concerning the reference trajectory (1), the arbitrary choice $K = 0.83$ has been made mainly to limit the overshoot while keeping good performances in terms of accuracy and response time. Finally, the function $\sigma(t)$ reads as

$$\sigma(t) = \frac{1}{1 + e^{-\lambda(t-t_0)}} \tag{20}$$

with $\lambda = 1$ and $t_0 = 0.15$ sec.
Remark that the definition (20) of $\sigma(t)$ fulfills $\sigma(0) \geq 0$ and small, $\sigma(t)$ monotonically increasing continuous and $\sigma(\infty) = 1$.

- **Scenario 1** (Figure 5) : The object is entered with a spherical grip. To allow a full grip, the effort is set to $15N$ and the object support is removed around 27 sec.
- **Scenario 2** (Figure 6) : The object is captured with a prismatic grip; as with the previous case, the effort is set at $15N$ and the coin support is removed around 32 sec.
- **Scenario 3** (Figure 7) : An egg is grasped by the three fingers with a force of $8N$ and the coin support is removed at 19 sec.

Taking into account the friction coefficient between the finger and the object, the value of 15 N is considered sufficient to hold any objects less than 500 g, within the range of available pressures. For a fragile object like egg, that force is reduced to 8 N. This value is set by the user as the control reference thanks to the knowledge of the object properties. In Figures 5, 6 and 7, the contact is indicated by a red dotted vertical line whereas the removal of the object support[7] is indicated by a black dotted vertical line.

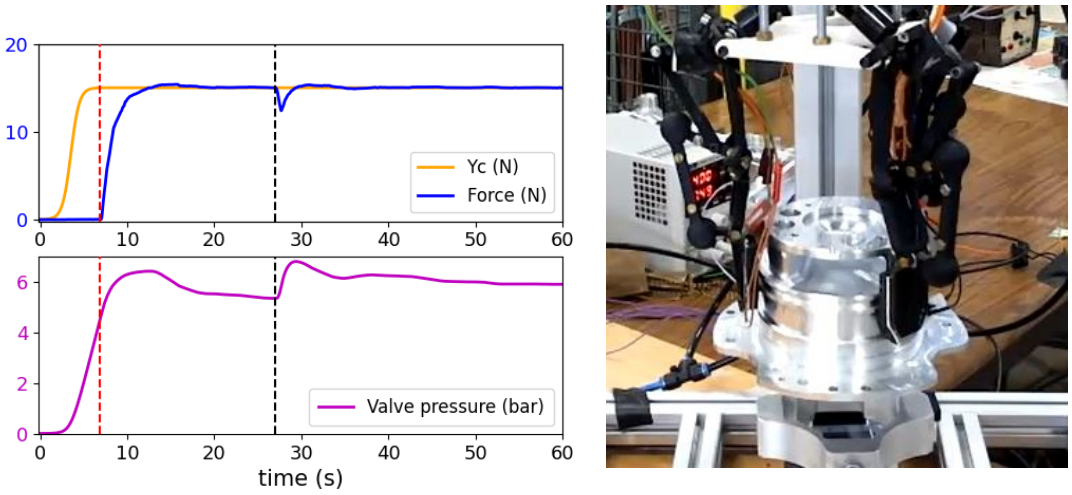

Figure 5: **Scenario 1. Left top.** Desired (yellow) and real (black) forces (N) versus time (sec). **Left bottom.** Pressure (bar) versus time (sec). **Right.** Photo of the experimental set-up with a spherical grip.

Each scenario shows that

- during *Phase 1*, the fingers are moving until contact with the object is made. Indeed, the pressure injected in the muscles is linearly increasing according to the time whereas the tracking error is decreasing and y keeps 0;

[7] During *Phase 3*, it is recalled that the object does not move and only the control changes to compensate for the lack of support.

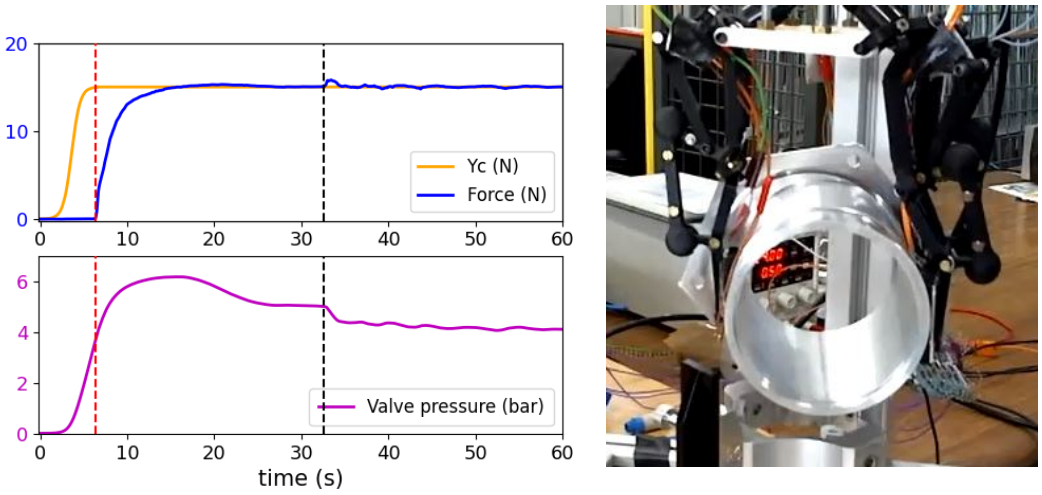

Figure 6: **Scenario 2. Left top.** Desired (yellow) and real (black) forces (N) versus time (sec). **Left bottom.** Pressure (bar) versus time (sec). **Right.** Photo of the experimental set-up with a prismatic grip.

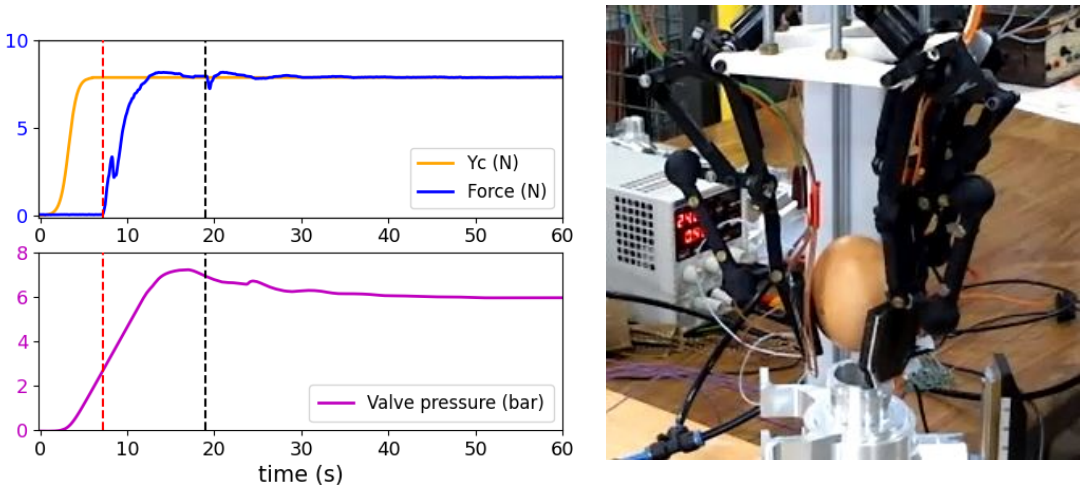

Figure 7: **Scenario 3. Left top.** Desired (yellow) and real (black) forces (N) versus time (sec). **Left bottom.** Pressure (bar) versus time (sec). **Right.** Photo of the experimental set-up grasping an egg.

- once the contact with the object is established (*Phase 2*), the pressure still increases to ensure accurate tracking between the force and its reference. During this phase, the underactuated fingers reach a position of stability [1] and create a grip of the object (shown by the next item, *i.e.* with the removal of the object support).
- grasping the object is illustrated with *Phase 3* during which the object is maintained in the fingers while the support is removed. Figures 5- 6-7 show that the force can either increase or decrease depending on the reactions applied to the object according to its geometry, which illustrates, in these cases, the benefits in using a model-free based control law.

In all three cases, the disturbance created by the removal of the support is rejected. The control shows good tracking of the reference when the object is in a free grip (without support). Notice that the low rigidity of the prototype limits a finer analysis of the results because the contact between the finger and the object is dampened and it is not possible to transmit significant forces. These first tests highlight the feasibility of the proposed approach and the relevance of the control architecture.

4.4. Repeatability and experimental asymptotic stability

The long-term stability of the grasping phase is experimentally studied, as well as the repeatability of the experiments. Figure 8-left illustrates the long-term stability of the measured force when the object is not moving. Due to the sensor drift, the hysteresis effect in the muscles, and the resulting force on the "measuring finger" (as a combination of the other forces applied to the object whose shape is unknown), the pressure injected into the muscles may vary to track the constant desired force, despite all nonlinear effects. To complete the experiments, Figure 8-right illustrates some tests that have been carried out (10 similar tests over 200 sec) to highlight some properties of repeatability of the force tracking efficiency despite different initial conditions/calibration of the force sensor.

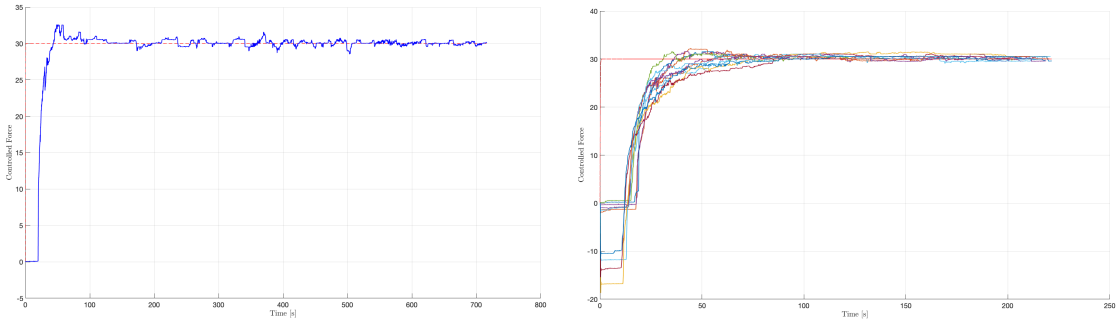

Figure 8: **Left.** Long-term experiment to verify the asymptotic stabilization of the grasping - Force (N) versus time (sec). **Right.** 10-time experiments to highlight the efficiency and the repeatability of the grasping - Force (N) versus time (sec).

4.5. About the performances of the precompensator

To highlight some properties of the precompensator, a study of the step response according to a set of values of the precompensator gain K (see equation 1) has been carried out, based on Scenario 1. The objective is to estimate the influence of K on the closed-loop system performance by the evaluation of certain standard parameters such as the overshoot, the static error, and the response time. Table 1 presents the results for $K = \{0, 0.5, 0.9\}$. The evaluation of the static error has been made on the time interval $t \in [100, 200]$ sec.

The precompensator is acting during the closing phase of the hand, the objective being to mitigate the contact force when the contact occurs, as detailed in Section 2.3. The main advantage of the precompensator is to slow down the approaching phase and the gain K allows adjusting the corresponding speed. The results presented in Table 1 show that the overshoot of the contact force is significantly damped if the gain K is large ($K = 0.9$). From (3), it can be explained by the fact that, the larger the gain K, the smaller the error e, and the less aggressive the controller

Gain K	Overshoot (%)	Static error $e(\infty)$ (N)	$t_{r5\%}$ (sec)
0	25.67	0.0020	8.09
0.5	8.09	0.0410	13.02
0.9	7.48	0.1386	36.47

Table 1: Control performances according to the gain K.

is. However, it can be noticed that the closed-loop system allows better accuracy and a smaller response time when K is small (ideally $K = 0$, but with a huge overshoot). As previously, it can be explained from (3) that the tracking error e is larger when K is larger, inducing a more aggressive controller.

5. Conclusions and future work

In this paper, a model-free control has been applied to a control scheme of a gripper composed of three fingers, each of them being actuated by a pneumatic muscle. The control scheme is based on a model-free approach and is using a reference continuous trajectory allowing to have no formal contact detection. Furthermore, no sophisticated model of the system, no knowledge of the object (except for the fact that it is symmetrical), and no trajectory planning are required. The experimental results demonstrate the feasibility and effectiveness of the proposed approach.
The main work to come concerns the design of a multivariable control scheme to separately control the three fingers in order to guarantee the mechanical stability even for asymmetrical objects. This class of control could allow for more efficient capture of a larger class of objects. Another future work is the use of robust control strategies that do not require models (for example, adaptive sliding mode control) in order to improve the tracking performances. Other gripping systems considering other shapes of objects as well as the installation of the gripper on a robotic arm will be investigated in further works.

Acknowledgment

The work has been supported by the French National Association for Research in Technology (ANRT) through the CIFRE 2019/27 and Armor Meca Developpement.

This research was supported by the project New smart and adaptive robotics solutions for personalized minimally invasive surgery in cancer treatment - ATHENA, funded by European Union – NextGenerationEU and Romanian Government, under National Recovery and Resilience Plan for Romania, contract no. 760072/23.05.2023, code CF 16/15.11.2022, through the Romanian Ministry of Research, Innovation and Digitalization, within Component 9, investment I8.

References

[1] P. Hamon, D. Chablat, F. Plestan, A new robotic hand based on the design of fingers with spatial motions, in: ASME 2021 International Design Engineering Technical Conferences and Computers and Information in Engineering Conference., Online, United States, 2021.
[2] L. Birglen, T. Laliberté, C. M. Gosselin, Underactuated robotic hands, Vol. 40, Springer, 2007.
[3] L. Birglen, T. Lalibert, C. M. Gosselin, Underactuated Robotic Hands, 1st Edition, Springer Publishing Company, Incorporated, 2010.

[4] B. Kalita, A. Leonessa, S. K. Dwivedy, A review on the development of pneumatic artificial muscle actuators: Force model and application, Actuators 11 (10) (2022).
[5] F. Sgarbi, J.-M. Detriche, Grab system actuated by a servo motor, european Patent EP0402229 (1989).
[6] Q. Xu, Design and smooth position/force switching control of a miniature gripper for automated microhandling, IEEE Transactions on Industrial Informatics 10 (2) (2013) 1023–1032.
[7] L. Birglen, C. M. Gosselin, Kinetostatic analysis of underactuated fingers, IEEE Transactions on Robotics and Automation 20 (2) (2004) 211–221.
[8] J. E. Takosoglu, P. A. Laski, S. Blasiak, G. Bracha, D. Pietrala, Determining the static characteristics of pneumatic muscles, Measurement and Control 49 (2) (2016) 62–71.
[9] B. Tondu, Modelling of the mckibben artificial muscle: A review, Journal of Intelligent Material Systems and Structures 23 (2012) 225 – 253.
[10] J. Takosoglu, Angular position control system of pneumatic artificial muscles, Open Engineering 10 (1) (2020) 681–687.
[11] W. Scaff, O. Horikawa, M. de Sales, Pneumatic artificial muscle optimal control with simulated annealing, in: 10th IFAC Symposium on Biological and Medical Systems BMS 2018, Vol. 51, Sao Paolo, Brazil, 2018, pp. 333–338.
[12] I. Godage, Y. Chen, I. Walker, Dynamic control of pneumatic muscle actuators, in: IEEE International Conference on Intelligent Robots and Systems, Madrid, Spain, 2018.
[13] T. D. C. Thanh, K. K. Ahn, Nonlinear pid control to improve the control performance of 2 axes pneumatic artificial muscle manipulator using neural network, Mechatronics 16 (9) (2006) 577–587.
[14] H. Pham Huy Anh, Online tuning gain scheduling mimo neural pid control of the 2-axes pneumatic artificial muscle (pam) robot arm, Expert Syst. Appl. 37 (2010) 6547–6560.
[15] J. Zhao, J. Zhong, J. Fan, Position control of a pneumatic muscle actuator using rbf neural network tuned pid controller, Mathematical Problems in Engineering 2015 (2015) 1–16.
[16] J. Zhong, X. Zhou, M. Luo, A new approach to modeling and controlling a pneumatic muscle actuator-driven setup using back propagation neural networks, Complexity 2018 (2018) 1–9.
[17] D. X. Ba, T. Q. Dinh, K. K. Ahn, An integrated intelligent nonlinear control method for a pneumatic artificial muscle, IEEE/ASME Transactions on Mechatronics 21 (4) (2016) 1835–1845.
[18] P. Hamon, L. Michel, F. Plestan, D. Chablat, Control of a gripper finger actuated by a pneumatic muscle: new schemes based on a model-free approach, IFAC-PapersOnLine 55 (27) (2022) 25–30, 9th IFAC Symposium on Mechatronic Systems MECHATRONICS 2022.
[19] M. Fliess, C. Join, Model-free control, International Journal of Control 86 (12) (2013) 2228–2252.
[20] M. Fliess, C. Join, An alternative to proportional-integral and proportional-integral-derivative regulators: Intelligent proportional-derivative regulators, Int J Robust Nonlinear Control (2021) 1–13.
[21] O. Bara, M. Fliess, C. Join, J. Day, S. M. Djouadi, Toward a model-free feedback control synthesis for treating acute inflammation, Journal of Theoretical Biology 448 (2018) 26–37.
[22] K. Hamiche, M. Fliess, C. Join, H. Abouaïssa, Bullwhip effect attenuation in supply chain management via control-theoretic tools and short-term forecasts: A preliminary study with an application to perishable inventories, in: 6th International Conference on Control, Decision and Information Technologies, CoDIT 2019, Vancouver, Canada, 2019.
[23] M. Bekcheva, C. Join, H. Mounier, Cascaded model-free control for trajectory tracking of quadrotors, in: International Conference on Unmanned Aircraft Systems, ICUAS'18, Dallas, TX, USA, 2018.
[24] Y. Younes, A. Drak, H. Noura, A. Rabhi, A. El hajjaji, Model-free control of a quadrotor vehicle, in: 2014 International Conference on Unmanned Aircraft Systems, ICUAS 2014, Orlando, FL, USA, 2014.
[25] J. Villagra, C. Join, R. Haber, M. Fliess, Model-free control for machine tools, in: 21st IFAC World Congress, IFAC 2020, Berlin, Germany, 2020.
[26] C. Sancak, M. Itik, T. T. Nguyen, Position control of a fully constrained planar cable-driven parallel robot with unknown or partially known dynamics, IEEE/ASME Transactions on Mechatronics 28 (3) (2023) 1605–1615.
[27] C. Sancak, F. Yamac, M. Itik, G. Alici, Force control of electro-active polymer actuators using model-free intelligent control, Journal of Intelligent Material Systems and Structures 32 (17) (2021) 2054–2065.
[28] P. Hamon, Conception et contrôle d'un préhenseur sous-actionné pour la saisie d'objets complexes, Ph.D. Thesis [in French], École Centrale de Nantes, France, 2022.
[29] K. J. Åström, R. M. Murray, Feedback Systems, Princeton University Press, 2008.
[30] B. d'Andréa Novel, M. Fliess, C. Join, H. Mounier, B. Steux, A mathematical explanation via "intelligent" pid controllers of the strange ubiquity of pids, in: 18th Mediterranean Conference on Control and Automation, MED'10, 2010, pp. 395–400.